The structural history of the Leipikvattnet Nappe in the Joma area of Nord Trøndelag, central Scandinavian Caledonides, Norway

NOELLE E. ODLING

Odling, N.E.: The structural history of the Leipikvattnet Nappe in the Joma area of Nord Trøndelag, central Scandinavian Caledonides, Norway. *Norsk Geologisk Tidsskrift*, Vol. 68, pp. 141–161. Oslo 1989. ISSN 0029–196X.

The Leipikvattnet Nappe in the Joma area is composed of the stratigraphic sequence, greenstone, quartzitic phyllite, graphitic phyllite, tectonically repeated by thrusting and locally overturned in the area of the Joma sulphide deposit. The greenstones (Røyrvik Group) are composed of massive and pillowed lava flows overlain by volcaniclastic deposits and are thought to represent the remnants of a basaltic sea mount or oceanic island. In the Joma area, D1 and D2 deformations are associated with movements on the major and internal thrust planes, whereas D3 and D4 postdate them. This sequence is correlated with deformation histories from the rest of the central Scandinavian Caledonides, using the major NE–SW trending folds to which the F3 Joma Synform belongs. D3 deformation is suggested, from lineation distributions and finite strain results, to have resulted from late movement of the Børgefjell massif. Subhorizontally oriented F4 folds are suggested to have formed in response to overburden pressure when horizontal stress was reduced over the crest of the rising massif.

Noelle E. Odling, Geologisk Institutt, N.T.H., Trondheim N7034, Norway; present address: IBM Bergen Scientific Centre, Thormøhlensgate 55, Bergen 5008, Norway.

The Leipikvattnet Nappe, one of the Köli Nappes in the Upper Allochthon of the Scandinavian Caledonides, crops out over a distance of approximately 120 km, trending NE–SW from the Grong–Olden Culmination to north of the Børgefjell massif (Fig. 1). The nappe contains the Joma massive sulphide deposit, situated 16 km east of the village of Røyrvik, Nord Trøndelag (Fig. 2), which is hosted by the Røyrvik Group greenstones and has been mined for Cu and Zn by Grong Gruber A/S since 1972. The present paper is based on a study of the structural history of the area immediately surrounding this massive sulphide occurrence, which falls within the bounds of 1:50,000 map-sheet, Jomafjellet (Fossen & Kollung 1988).

In the vicinity of the Joma deposit, the Leipikvattnet Nappe is composed of intercalated greenstone, quartzitic phyllite and graphitic phyllite units (Fig. 2). The rocks show evidence of four deformation phases. The dominant phase (D2) has resulted in a largely penetrative schistosity subparallel to the lithological layering, and is associated with major movements on thrust planes. Evidence of an earlier phase, largely overprinted by D2 deformation, is locally preserved in quartzitic phyllites. The penetrative schistosity and thrust planes are folded by the third phase of deformation, to which the major, NE–SW trending Joma Synform belongs, giving the characteristic arcuate form to the outcrop pattern. A fourth phase of deformation, comprising minor folds and kinks, is weakly developed in the south of the area adjacent to the upper bounding thrust of the Leipikvattnet Nappe. This sequence of deformation is in agreement with the general scheme of deformation present throughout the Upper Allochthon of the central Scandinavian Caledonides (Zachrisson 1969; Trouw 1973; Halls et al. 1977; Stephens 1977; Sjøstrand 1978; Aukes et al. 1979; Kollung 1979; Lutro 1979; Roberts 1979; Sandwall 1981).

The Geology of the Joma area

The rocks of the Leipikvattnet Nappe in the Joma area comprise intercalated units of graphitic and quartzitic phyllites and greenstones. Greenstone (named the lower, middle and upper greenstones) occurs at three structural levels which are grossly similar but show individual characteristics. The

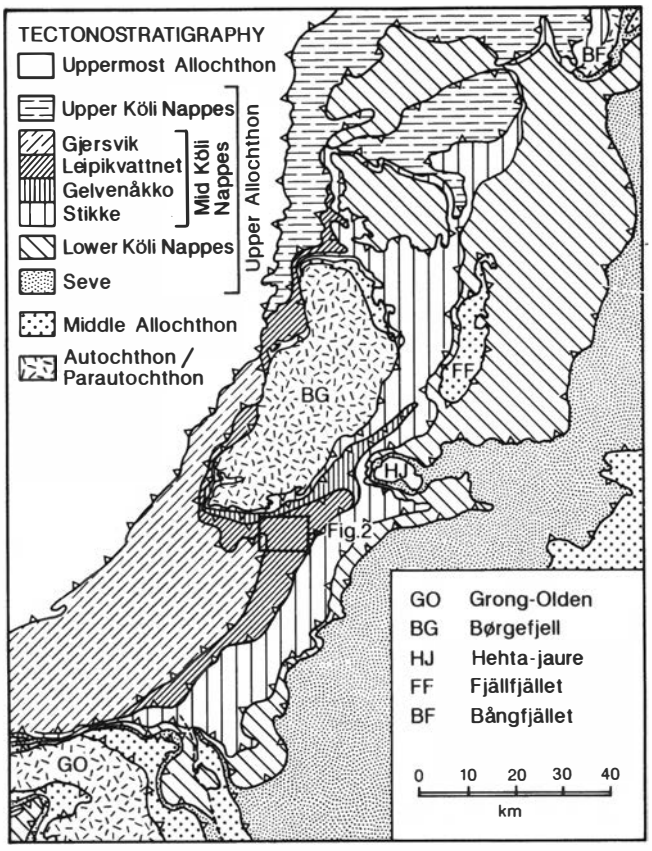

Fig. 1. Map of the central Scandinavian Caledonides after Stephens & Gee (1985), Häggbom (1978), Ramberg (1981) and Reinsbakken (unpublished data). The Leipikvattnet Nappe outcrops over a distance of 120 km from north of the Grong–Olden Culmination to north of the Børgefjell massif. Location of Fig. 2 showing the Joma area is outlined.

term greenstone is used in this paper in a purely descriptive sense and includes all hornblende-, actinolite- and/or chlorite-rich rocks which may be of extrusive or intrusive igneous or volcaniclastic origin.

The lower greenstone

The lower greenstone is composed of pillow lavas and massive greenstones. The pillow lavas show well-preserved pillow structures with dark, fine-grained rims and paler cores with abundant fractures filled largely by carbonate. The pillows are closely packed, with sparse interstitial sediments. Adjacent to the upper contact of the lower greenstone with quartzitic phyllites, the pillows contain variolitic structures comprising spherical to ellipsoidal particles from 2 mm to 4 cm long. These show internal concentrical layering and are mineralogically similar to the host greenstone but contain higher proportions of clinozoisite.

Pillowed greenstone is dominant in the east and passes westwards, through a complexly interfingered zone (Fig. 2), into a massive greenstone of varying grain size which, in the coarsest examples, displays relict ophitic textures. Grain size of this massive greenstone was found to be independent of deformation intensity and the variation is therefore thought to be an original feature. The massive greenstone has sharp or gradational contacts with pillow lavas and, where gradational, passes into pillow lavas through a breccia composed of pillow fragments. The relict ophitic textures indicate an igneous origin for the massive greenstone which is interpreted as representing massive flows and shallow-level intrusions. Associated with the massive greenstones are thin lenses of black graphitic and quartzitic phyllite which commonly show an *en échelon* arrangement. These closely resemble the phyllites that separate the three greenstone units and are associated with breccias containing greenstone fragments and impure marbles.

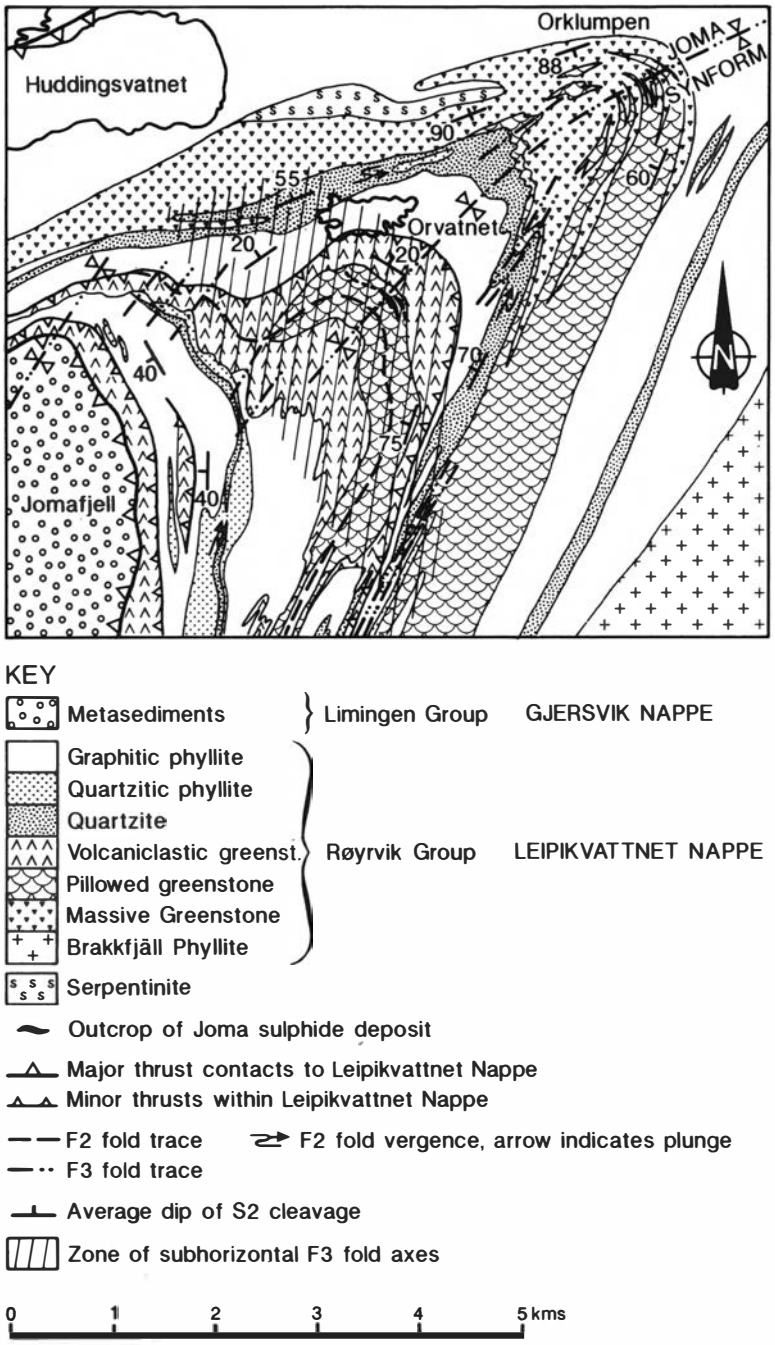

Fig. 2. Geological map of the Joma area, adapted from Kollung (1979) and Fossen & Kollung (1988) with additional mapping by the present author.

The middle greenstone

The pillow lavas of the middle greenstone closely resemble those of the lower greenstone, except that no variolitic structures were found and interstitial sediments are more abundant. They, however, show a generally lower state of preservation than the pillow lavas of the lower greenstone,

pillow margins being generally difficult to identify or completely obliterated. From examination of pillow lavas in varying states of preservation, it was found that they are characterized by the presence of elongate lenses of intense fracturing which are frequently calcite filled. These have weathered to give a characteristic appearance which was used to identify the pillow lavas where all signs of pillow margins have been destroyed.

The pillow lavas were found to form an elongate wedge-shaped outcrop in the centre of the middle greenstone (Fig. 2), which is flanked by massive to finely laminated greenstones. This laminated greenstone, which resembles the interstitial sediments between pillows, is composed of light and dark laminae formed by varying proportions of plagioclase, actinolite and clinozoisite, which are the constituent minerals of the greenstone, and is interpreted as a volcaniclastic deposit. Intercalated with laminated greenstones are more massive units which show only faint layering. Due to the presence of layering, their concordance with laminated greenstone and the lack of any igneous textures, these are also thought to be of volcaniclastic origin.

The upper greenstone

The upper greenstone forms discontinuous layers adjacent to the upper bounding thrust to the Leipikvattnet Nappe. It is largely composed of medium- to fine-grained, massive greenstones but also contains laminated greenstone which closely resembles the volcaniclastic sediments of the middle greenstone. This, together with the lack of any relict igneous features, is thought to indicate that these greenstones also represent volcaniclastic sediments similar to those of the middle greenstone.

The phyllites

Quartzitic phyllites are concentrated near the structurally upper contacts of the lower and middle greenstones. They show gradational contacts with graphitic phyllites, and the name 'quartzitic phyllite' was arbitrarily applied by Kollung (1979) to phyllites with more than about 50% quartz. The quartzitic phyllites are composed of alternating quartz-rich and mica-rich layers. The quartz-rich layers range from a few mm to 10 cm thick and show a complete gradation from laterally continuous, parallel layers of even thickness and separation to anastomosing, discontinuous layers down to a few mm thick. As the earliest fold structures were found in quartzitic phyllites with regular layering, it is thought likely that this type of layering is an original feature from which the irregular, anastomosing layering is developed by deformation. The competence contrast between graphitic and quartz-rich layers renders the rock susceptible to folding and this rock type is the most sensitive indicator of the deformation history in the area. In contrast to the quartzitic phyllites, which are resistant to erosion and form high standing ground, the graphitic phyllites are susceptible to weathering and are poorly exposed. They resemble the mica-rich layers within the quartzitic phyllites.

The deformation history of the Leipikvattnet Nappe

In the following section, deformation phases are denoted as D1 to D4, fold generations as F1 to F4, schistosities and cleavages as S1 to S4 and lineations as L1 to L4. As the sequence of phases has been determined by the relationship of structures to those of the dominant deformation phase, this dominant phase (D2) has been described first and is followed by descriptions of D1, D3 and D4.

Main phase deformation – D2

The main penetrative schistosity and mineral lineation developed in the area belong to the second identifiable phase of deformation. S2 schistosity dips SW to NW (due to later folding), forming a distribution that approximates a great-circle about the major F3 fold axis (Fig. 3a). Mineral lineations in the graphitic phyllites and greenstones and rodding lineations on quartz layers within quartzitic phyllites dip gently NW/SW to NE (Fig. 3b). F2 folding is best developed in the quartzitic phyllites, where it is commonly refolded by F3 folds. However, where F3 folding is gentle, it was possible to determine the vergence of F2 folds. The sense of vergence in the quartzitic phyllites overlying the lower and middle greenstones was found generally to be similar. After 'unfolding' the Joma Synform, this is sinistral looking eastwards along the F2 axes.

In the greenstone units, F2 folding is rarely developed and the intensity of D2 deformation is

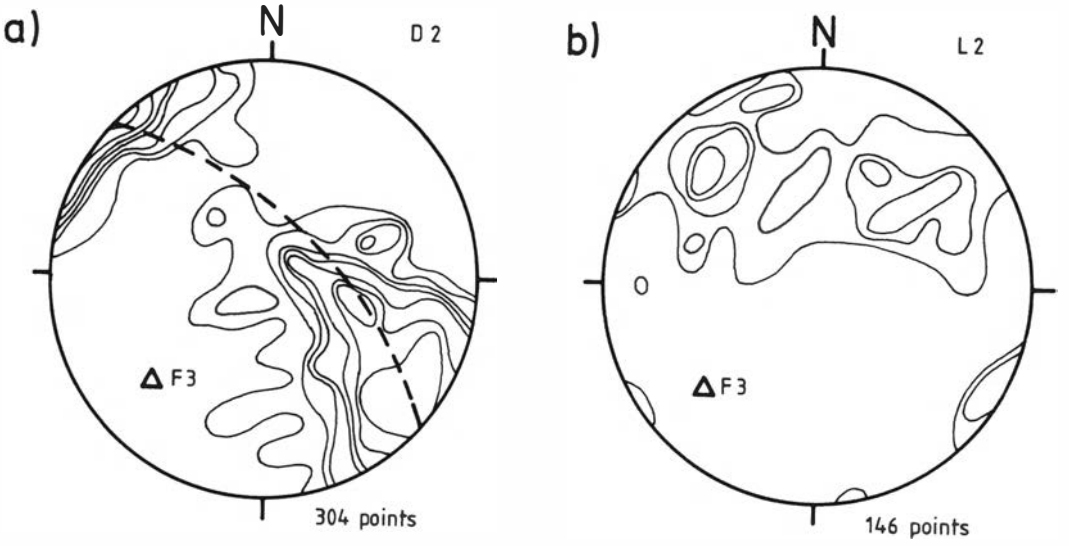

Fig. 3. (a) Stereoplot of poles to S2 schistosity and F2 axial planes. The distribution approximates a great circle whose pole approximates the fold axis of the F3 Joma Synform. (b) Stereoplot of L2 lineations (mineral and rodding lineations, F2 fold axes) which plunge gently NW/SE to NE. Contours at 2, 4, 6, 8, 10, 15 and 20 points per 1% area.

reflected by the S2 schistosity strength. The relative intensities of S2 schistosity, mapped in the middle greenstone, show that S2 is most strongly developed adjacent to the lower contact and weakest in the centre of this greenstone unit (Fig. 4). At rare exposures of the structurally lower contacts of the middle and upper greenstone units (around locality at VM472907), S2 schistosity within the greenstone was seen to be slightly oblique to the contact and to increase in intensity and swing into parallelism approaching the contact (Fig. 5). In a few places, layering in quartzitic phyllites was observed to be truncated by the contact (Fig. 5) and, at the lower contact of the upper greenstone unit, many thin intercalated slivers of greenstone and phyllite were seen. These features are thought to indicate that these contacts are tectonic in origin and that they mark the locations of secondary thrusts within the Leipikvattnet Nappe. The distribution of S2 schistosity intensity within the lower greenstone shows a rather different pattern to that of the middle greenstone, being most strongly developed in the thin western limb and decreasing in intensity eastwards. The lower contact was nowhere found exposed and it is therefore uncertain whether it also marks the location of a thrust. However, the similarity in outcrop pattern with the middle greenstone suggests that it may also be of a tectonic nature.

The repeated sequence of greenstone, quartzitic phyllite and graphitic phyllite is thus interpreted as a structural repetition resulting from movement along thrusts internal to the Leipikvattnet Nappe which are located at the structural bases of the middle and upper greenstones and possibly also the lower greenstone. The relationship between S2 schistosity and the lower contacts of the greenstones indicates that the movement is associated with D2 deformation and therefore coeval with movement along the major thrusts bounding the Leipikvattnet Nappe.

At the level of present-day exposure, the area of low D2 deformation in the middle greenstone coincides approximately with the distribution of pillowed greenstone which outcrops in a thin, elongate wedge, trending parallel to the trace of S2 schistosity (Fig. 4). This, together with the similarity of the laminated greenstones exposed on either side, suggests the presence of a major F2 fold whose trace passes through the outcrop of pillowed greenstone. Further evidence of this fold was found from lithological logging of drill-cores located along an east–west profile by Reinsbakken (1986a). Three major lithological types were identified by Reinsbakken; pre- and post-ore pillowed sequences, distinguished on the basis of mineralogy and chemistry, and a volcaniclastic greenstone. Their distribution shows a repeated sequence reflected about the location of the pro-

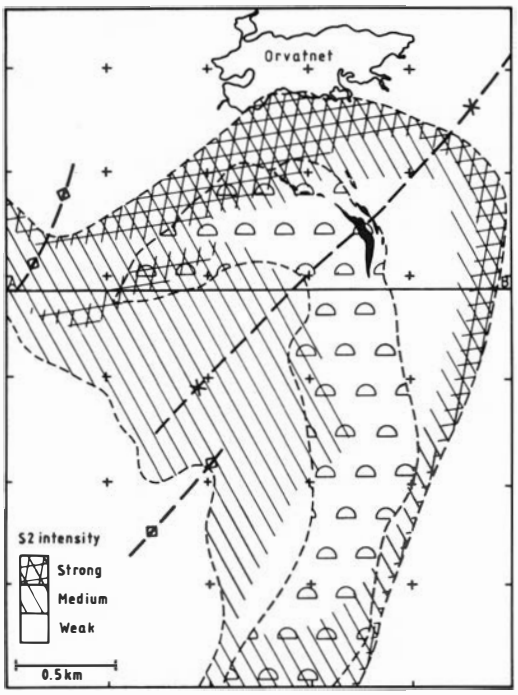

Fig. 4. Map of D2 deformation intensity in the middle greenstone, estimated from S2 schistosity development. The categories of schistosity development were defined as follows: strong – well-developed parallel alignment of amphiboles and micas and almost total destruction of original features such as pillow outlines and volcaniclastic layering; medium – partial alignment of amphiboles and micas with original features still discernible although elongated; weak – very poorly developed to no alignment of amphiboles and micas with no discernible deformation of original features. Deformation is most intense adjacent to the greenstone lower contact and least intense in the vicinity of the pillow lava outcrop (ornamented). The line A–B shows the location of the cross-section in Fig. 6.

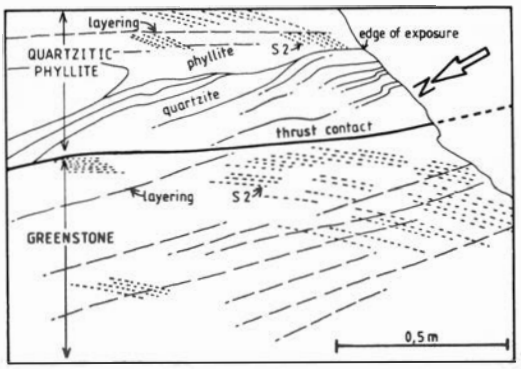

Fig. 5. Sketch from a photograph of the thrust contact (plan view) at the base of the middle greenstone on the eastern limb of the Joma Synform (UTM coordinates VM472907). S2 schistosity swings to become parallel approaching the contact and layering in the quartzitic phyllites is obliquely cut by the contact.

posed F2 fold trace, which is truncated at depth by the contact at the base of the middle greenstone (Fig. 6). This provides further evidence that the lower contact of the middle greenstone is the location of a thrust. Both the F2 fold trace and the thrust at the base of the middle greenstone are refolded by the F3 Joma Synform.

The outcrop pattern implies that the Joma massive sulphide deposit occurs in the structurally lower limb of this fold and this is consistent with the vergence of F2 folds found in the ore body (Odling 1988), which is opposite to that of the quartzitic phyllites. This pattern of F2 fold vergence implies that the fold is antiformal. Previous studies of stratigraphy and chemistry of the sulphides and surrounding greenstones have indicated that the ore body, interpreted to be of exhalative origin, is inverted (Olsen 1980; Reinsbakken 1986b). This sense of younging thus implies that the stratigraphy is locally inverted only in the region of the ore body and that the upper portion of the middle greenstone is the correct way up. As there is no indication of further major F2 folds between the thrusts at the base of the middle and upper greenstones, this therefore suggests that the structurally repeated sequence, greenstone, quartzitic phyllite, graphitic phyllite, represents a *stratigraphic* sequence.

The presence of other major F2 fold traces within the Joma area is not suspected. The lower greenstone has a superficially similar outcrop pattern to that of the middle greenstone (Fig. 2) but, due to a lack of any relationship between the outcrop pattern and the intensity of D2 deformation, this is thought to be an original feature. It is not known if any major F2 folds exist within the upper greenstone as, although it has a well developed schistosity, it lacks marker horizons. However, since this greenstone outcrops only as a thin strip adjacent to upper bounding thrust of the Leipikvattnet Nappe, any F2 folds within this greenstone unit would affect the younging direction of only a small portion of the Leipikvattnet Nappe in this area. It is thought, therefore, that the rocks of the Leipikvattnet Nappe in the Joma area are generally the right way up except where locally overturned by F2 folding in the area of the Joma sulphide deposit.

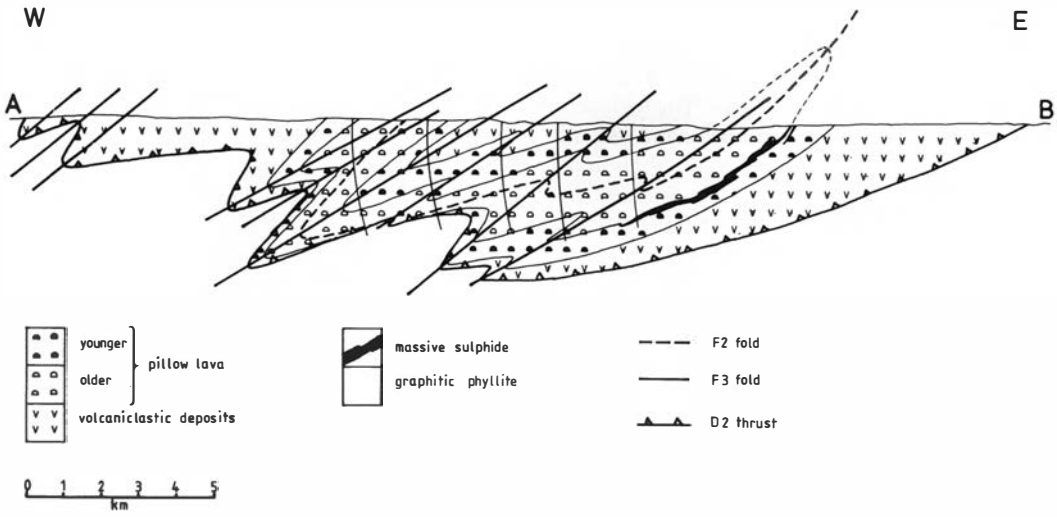

Fig. 6. Structural cross-section A–B (location shown in Fig. 4) through the middle greenstone, constructed from long drill holes logged by A. Reinsbakken (Reinsbakken 1986). The greenstone lithologies are reflected about an F2 fold trace and refolded by the F3 Joma Synform. The Joma sulphide deposit lies on the F2 fold lower limb and both the deposit and the fold are cut by the thrust at the base of the middle greenstone.

Early deformation – D1

F1 folds were identified in thin sections and sporadic outcrops of quartzitic phyllite. They appear as small-scale folds, with an axial planar penetrative schistosity in the mica-rich layers, which is strongly crenulated by S2 and more gently folded by F3 folds (Fig. 7). The interference fold patterns and lineations on quartz layers suggest that F1 and F2 folds are coaxial. Further evidence of a deformation prior to the main phase D2 was seen in the Joma sulphide deposit. Tectonic contacts between greenstone and sulphide were observed to be folded around large F2 fold hinges, implying that at least some of these contacts must have developed prior to D2 (Odling 1988; Marshall in press). This deformation is correlated with the D1 deformation phase identified in the quartzitic phyllites.

Within the greenstone units, no indication was found of deformation earlier than D2. Where the S2 schistosity is weakly developed, the original features of the greenstone (pillows, breccia fragments) can be identified and S2 is nowhere observed as a crenulation of an earlier cleavage or schistosity. This, together with the probability that F1 and F2 folds in the quartzitic phyllites are coaxial, suggests that D1 and D2 deformations represent essentially early and late structures within the same deformation phase. The dif-

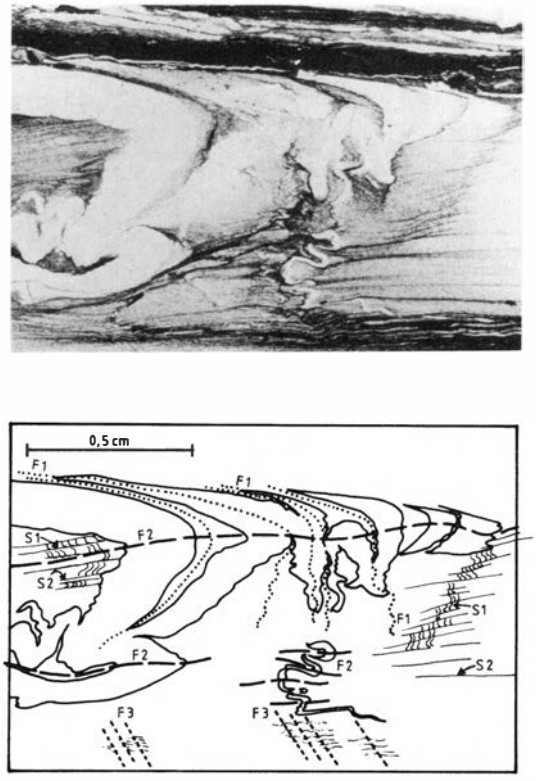

Fig. 7. Microphotograph and sketch of F1, F2 and F3 folds in a thin section of quartzitic phyllite (UTM coordinates VM471939).

ference between the quartzitic phyllites and greenstones in recording the early deformation can be explained in terms of the mechanical properties of these two rock types. The high competency contrast between quartzitic and phyllitic layers in the quartzitic phyllites results in the early development of folds which can be refolded at a later stage in the deformation. In the greenstones, which generally lack layering of contrasting competency, the effect of further deformation on an early developed schistosity is simply to strengthen it so that early and late deformations are indistinguishable.

D3 deformation – the Joma Synform

Thrust planes of D2 age and S2 schistosity are folded by the major, NE–SW trending D3 Joma Synform which gives the arcuate outcrop pattern characteristic of the Joma region (Fig. 2). This synform, which plunges either gently SW or NE, has a steeply west to NW dipping eastern limb and a gently SE to steeply NW dipping western limb. The interlimb angle of this major fold increases to the SW, where the fold dies out as another NE–SW trending synform is developed to the NW in the overlying Gjersvik Nappe (Fig. 2).

D3 deformation intensity, highly variable throughout the region, is most strongly developed around the inner arcs of the lower and middle greenstones in the Joma Synform hinge zone, the steeply dipping eastern limb, and the western limb where it dips steeply NW. F3 folds are open to tight, commonly with a near chevron style, to which S3 forms an axial planar crenulation cleavage, rarely penetrative. Small-scale F3 folds are commonly discontinuous along their traces (as is the major Joma Synform) and tend to occur in groups forming zones of F3 folds which are distributed in *en échelon* or relay patterns. F3 folds trend at approximately right angles to F2 fold hinges, thus developing characteristic dome-and-basin interference fold patterns in the quartzitic phyllites.

S3 crenulation cleavage and F3 fold axial planes dip moderately NW and are slightly steeper on the SE limb of the Joma Synform, reflecting a slight fanning around the major fold hinge (Fig. 8). F3 fold hinges and L3 intersection lineations vary in plunge from gently SW to gently NE forming NW–SE trending zones of L3 plunge

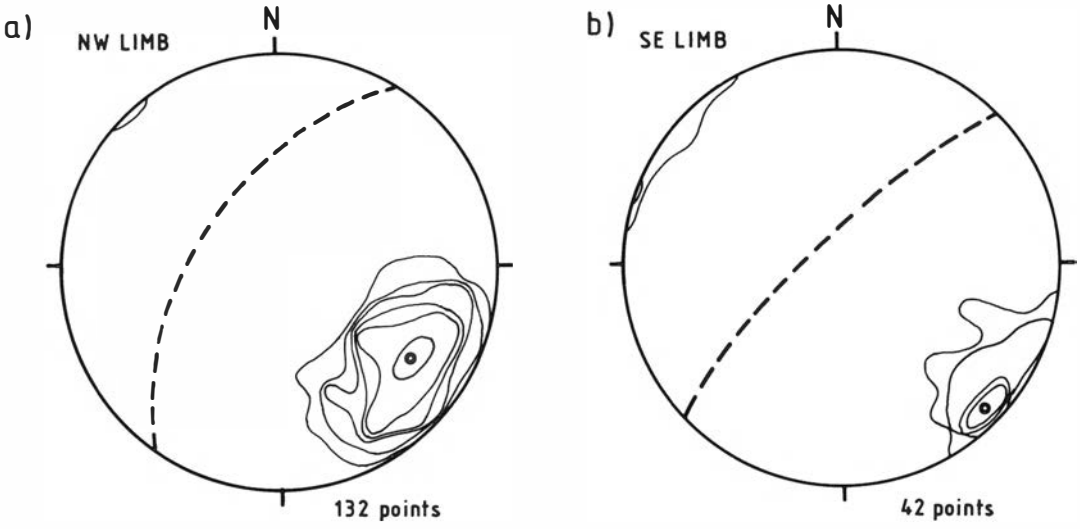

Fig. 8. Stereoplots of D3 planar structures (S3 crenulation cleavage and F3 fold axial planes) on (a) the NW limb and (b) the SE limb of the Joma Synform. Contours at 2, 4, 6, 8, 10 and 20 points per 1% area.

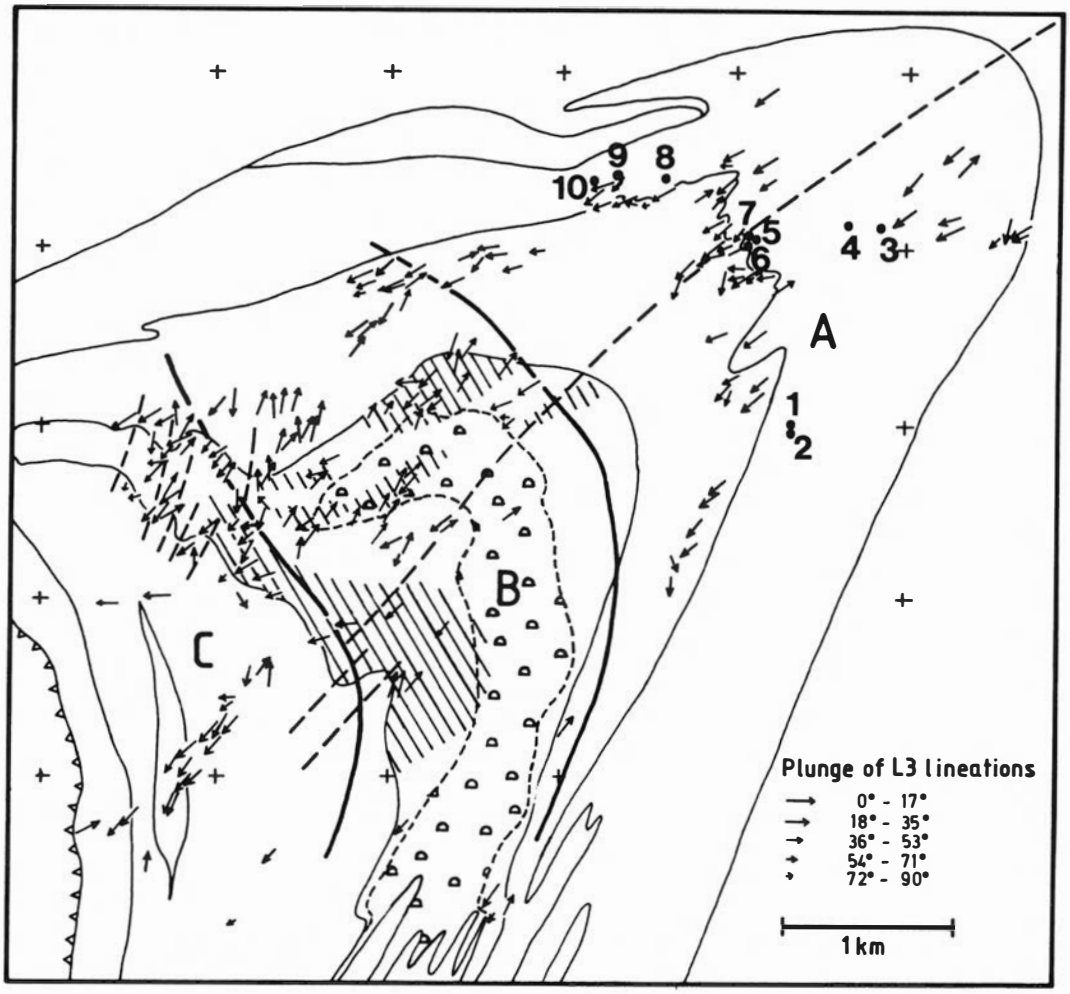

Fig. 9. Map showing the variation in L3 plunge in the Joma area and D3 deformation intensity (lined ornament) in the middle greenstone. L3 lineations plunge gently SW in areas A and C, and subhorizontally to gently NE in area B. D3 deformation is most intense in the inner arc and the NW limb of the Joma Synform within the middle greenstone. Black dots show the localities of variolitic greenstone specimens used in the estimation of finite strain.

direction. Southwesterly plunges occur in the SW and NE of the area (zones A and C, Figs. 9 and 10) and are separated by a zone of NE plunges in the region of the middle greenstone (zone B, Figs. 9 and 10). The cause of this variation in L3 plunge could be one of three alternatives; post-D3 deformation, variable intensity of D3 deformation or a variation in the pre-D3 surface (S2 and lithological layering). As D4 structures are very weakly developed in the area, it is unlikely that later deformation could have significantly affected the L3 plunge. Although D3 deformation is variable in intensity, areas of strong F3 folding and well-developed S3 cleavage trend NE rather than NW (Fig. 9) and cut across zone B of NE, L3 plunges. It is thought most probable, therefore, that the variation in L3 plunge is due to variation in the orientation of S2 cleavage and lithological layering prior to D3 deformation.

The F3 Joma Synform has folded the NW–SE trending, L2 lineations. The distribution of folded lineations is dependent on the type of deformation active during folding (Ramsay 1967). Thus these L2 distributions can be used to give information on the D3 folding mechanism by comparing simple theoretical models with the observed distributions. The possible theoretical distributions of folded lineations can be represented

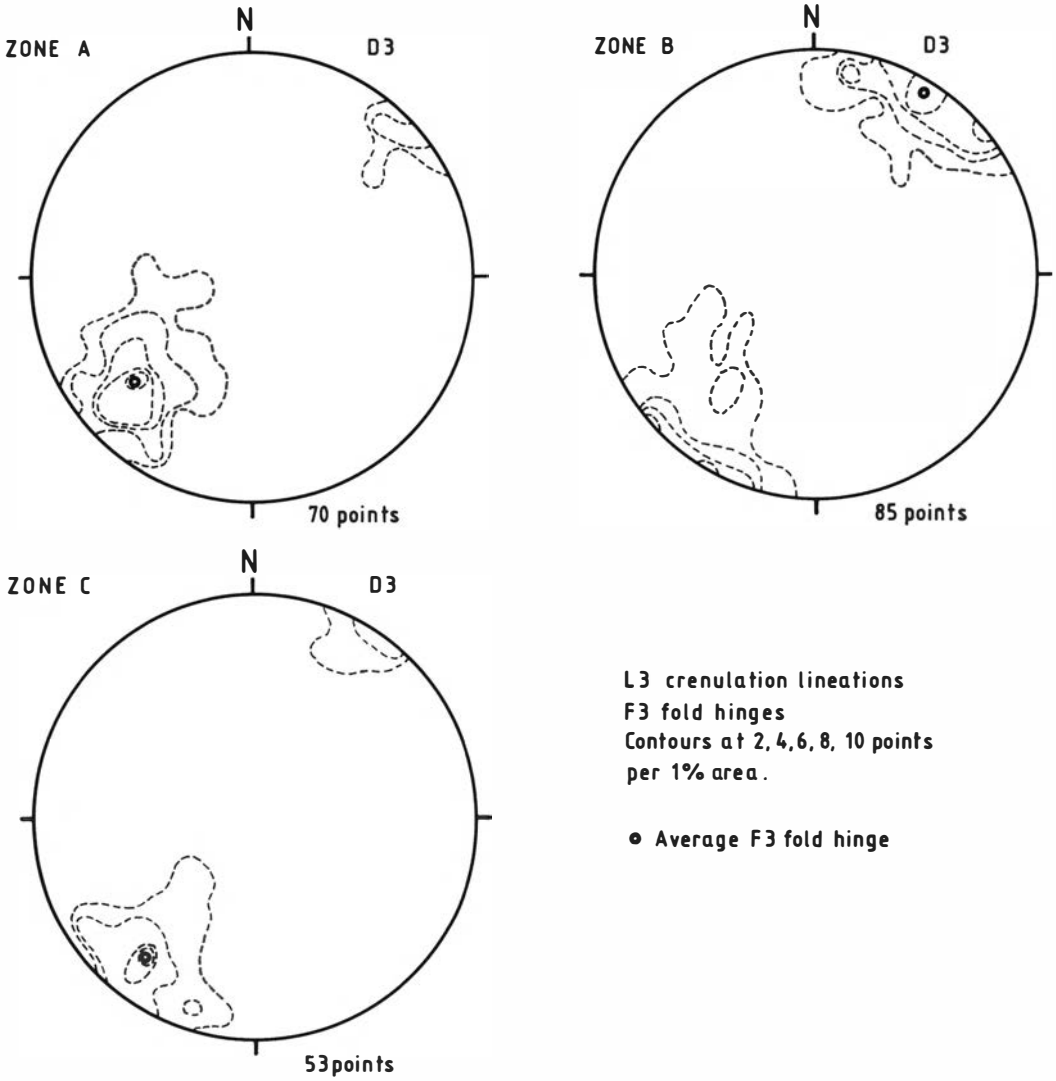

Fig. 10. Stereoplots of L3 lineations for areas A, B and C shown in Fig. 9. L3 lineations plunge gently SW (averages of 30° and 20°, respectively) in areas A and C, and subhorizontally to gently NE (average of 8°) in area B. Contours at 2, 4, 6, 8 and 10 points per 1% area.

by those formed by two end-member folding mechanisms; concentric and simple shear folding. Concentric folding results in small-circle distributions about the fold axis and shear folding results in great-circle distributions containing the original lineation orientation and the shear direction (Ramsay 1967, ch. 8). The original, pre-D3 orientation of L2 is uncertain, but an estimate was obtained from the hinge zones in 'box-shaped' F3 folds in the quartzitic phyllites, where the pre-D3 orientation of L2 is thought to be undisturbed. This gives a shallowly NW-plunging lineation direction as the pre-D3, L2 lineation orientation. Assuming that L2 parallels the D2 shear direction, this is in agreement with the overall gentle westerly dip of the nappes of the Upper Allochthon. The shear folding model was constructed using the best-fit great-circle to the L2 distributions for zones A, B and C, that passes through the estimated original orientation of L2 (Fig. 11). For the concentric folding model, the small-circles traced by the estimated pre-D3, L2 orientation

about the F3 fold hinge (determined from the maxima of L3 orientations) were constructed (Fig. 11).

Plots of L2 distribution for these three zones A, B and C (Fig. 11) show that there is no significant variation in the L2 patterns among these zones. As the average F3 fold axis directions in zones A and C are close to perpendicular to the F2 trend, concentric and simple shear models give similar results and show equally good fits to the L2 distribution. However, in zone B, the average F3 axis is oblique to the F2 trend and the two models give rise to different folded lineation patterns. Here the simple shear model shows by far the better fit to the L2 lineation distribution (Fig. 11). It is possible that the L2 lineation distribution produced by the concentric folding model could be modified to provide a better fit to the observed data by additional pure shear. However, any pure shear component that would alter the L2 lineation distribution in the desired fashion would also tend to steepen minor F3 hinges. As these have

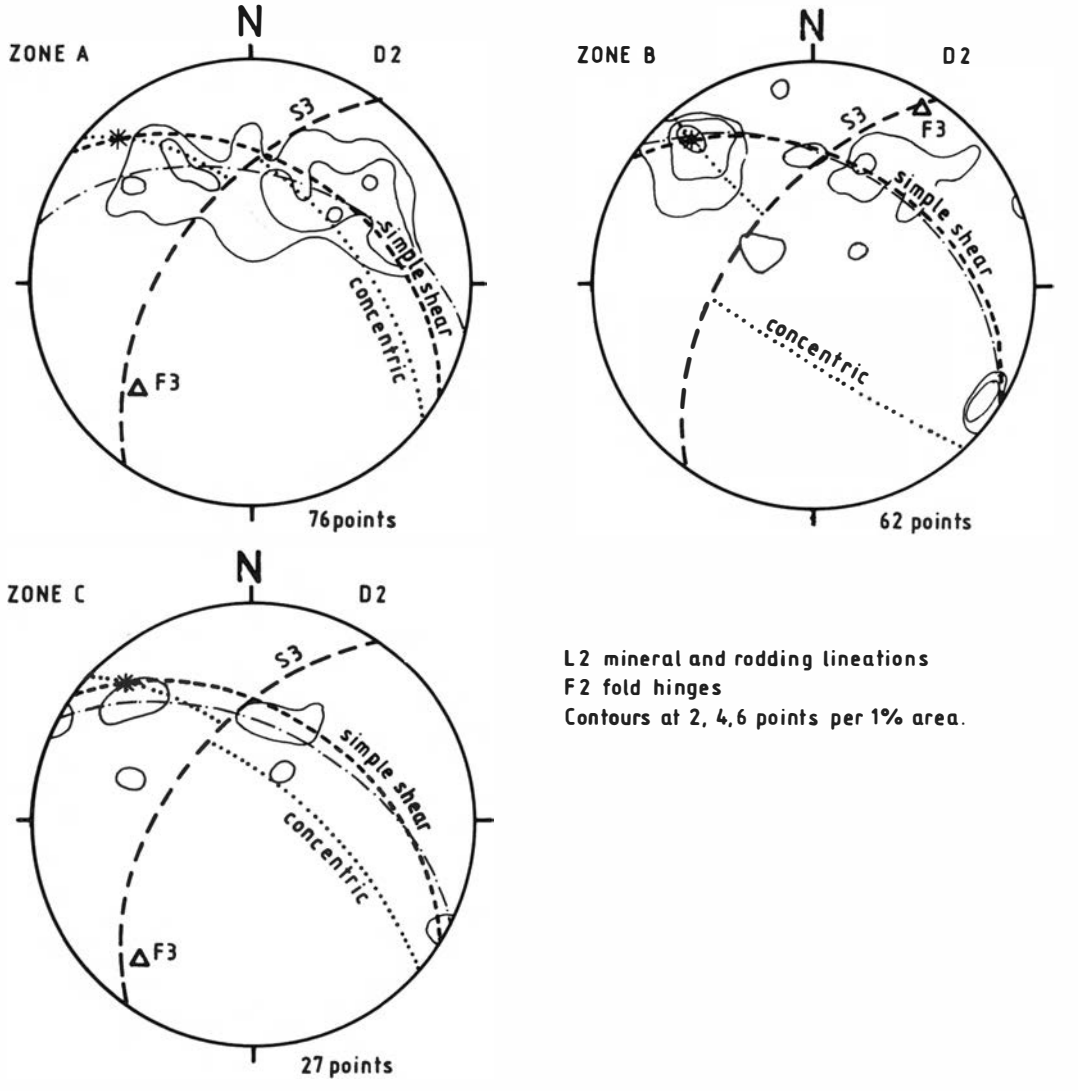

Fig. 11. Stereoplots of L2 lineation distributions in areas A, B and C and the theoretically expected distributions produced by simple shear (dashed line) and concentric (dotted line) folding. The best fit great circle to the observed data is marked by a dash-dot line. The data fit both folding models equally well for zones A and C, but in zone B only the shear folding model gives a distribution similar to that observed. Contours at 2, 4, 6, 8, 10, 15 and 20 points per 1% area.

remained subhorizontal, it seems unlikely that significant compression of the required orientation can have taken place. The distribution of L2 lineations in zone B therefore suggests that F3 folding developed by a dominantly simple shear mechanism.

Significance of the greenstone outcrop pattern in the Joma area

Lithological and structural mapping has shown that the three greenstone layers of the Joma area probably represent tectonically repeated segments of an originally single horizon which was composed of massive and pillowed flows and volcaniclastic sediments. The greenstone layers show a marked thickening of their outcrop in the core of the Joma Synform. Both the middle and lower greenstones thin and finally disappear against probable thrusts southwards along the east limb of the Joma Synform while to the west the greenstone horizons become thin and are composed of numerous horizons intercalated with phyllites. This thickening was attributed by Kollung (1979) to deformation associated with the Joma Synform (D3). However, detailed structural mapping of the greenstone units has shown no correlation of the outcrop pattern with the intensity of either D2 or D3 deformation. This, together with the change in outcrop characteristics along strike, is thought to indicate that the outcrop shape reflects an original thickness variation. Returning the three layers of greenstone to their probable original relative positions by transporting the middle and upper greenstone eastwards of the lower greenstone would suggest that, originally, the massive lavas graded laterally into pillowed lavas which are overlain by volcaniclastic sediments.

Chemical analysis of the Joma pillowed greenstones by Olsen (1980), Stephens et al. (1985a) and Reinsbakken (1986b) and their association with layered quartzitic phyllites, tentatively interpreted as recrystallized ribbon cherts (Reinsbakken in Stephens & Reinsbakken 1981; Stephens 1986), fine-grained sediments and the Joma massive sulphides deposit which is interpreted to be of exhalative origin (Olsen 1980; Reinsbakken 1986b), has led to the suggestion that they represent tholeiitic to alkaline basalts with affinities similar to mid-ocean-ridge and within-plate basalts. Olsen (1980) originally interpreted them as representing a back-arc basin, but subsequent data from the Middle Köli has led Stephens & Gee (1985) to interpret the Røyrvik Group of the Leipikvattnet Nappe and the Remdalen Group of the Stikke and Gelvenåkko Nappes as representing the ocean floor on which the island arc, represented by the Gjersvik igneous complex, was developed. They thus interpret the Joma pillowed lavas as representing the top layer of ocean floor in a probably off-axis situation. Within the framework of this interpretation, the thick portions of the Røyrvik Greenstones in the core of the Joma Synform may represent the remnants of a seamount or ocean island with which the deposition of the Joma massive sulphide deposit was associated.

D4 deformation

Late-phase D4 deformation within the Leipikvattnet Nappe in the Joma area is expressed as conjugate sets of minor kink folds which occur sporadically but are concentrated in the SW, adjacent to the thrust contact with the Gjersvik Nappe. Axial plane orientations are highly variable (Fig. 12) but conjugate set intersections consistently plunge subhorizontally with NE–SW trends (Fig. 12). The geometry of the kink folds indicates an overall moderate to steep NW-plunging direction of maximum compression.

In the Joma area, D3 and D4 structures were found to show a complementary spatial relationship. Approaching the upper bounding thrust of the Leipikvattnet Nappe, D3 deformation becomes less intense while D4 structures become more widespread. In the overlying Gjersvik Nappe within the area of Fig. 2, no F3 folds were identified and the shallowly dipping member of the F4 conjugate set becomes dominant. Where both F3 and F4 structures occur, F4 postdate F3 folds, but the spatial relationship between the two phases of deformation suggests a close relationship and it is thought that D4 deformation probably followed D3 within a short time interval.

Strain analysis

Estimation of finite strain was carried out to aid in the interpretation of the mechanisms that gave rise to the various deformation phases. Variolitic structures which occur widely throughout the pillow lavas of the lower greenstone, and for which relatively small samples sufficed, were used as strain markers. The pillow lavas themselves were

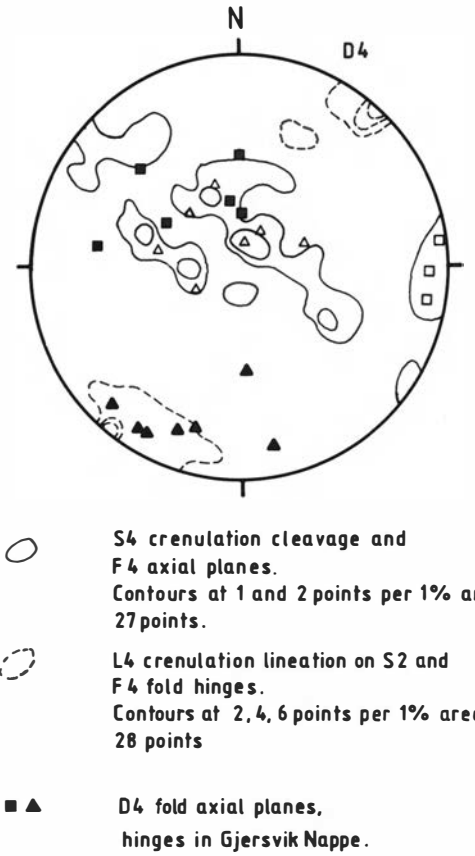

Fig. 12. Stereoplot showing D4 planar and linear minor structures in the Leipikvattnet Nappe (contoured) and Gjersvik Nappe (solid symbols). Open symbols show conjugate sets in Leipikvattnet Nappe.

generally found to be too poorly preserved and exposed to be practical as strain markers.

The variolitic structures found in the lower greenstones occur in groups of subspherical to ellipsoidal particles (Fig. 13). The varioles are 1 mm to 10 cm in length, and are composed of concentric layers rich in actinolite, plagioclase, clinozoisite and sphene. They may be either paler or darker than their matrix, depending on the relative concentrations of clinozoisite and sphene. The origin of these structures is unknown, but their location within pillows, the observation that the groups do not cross pillow margins, and the correspondence between their elongation and intensity of S2 schistosity suggests that they are an original feature of the pillowed greenstone. The similarity of shape shown by varioles from the same locality suggests that they were originally approximately spherical and this is supported by

Fig. 13. Microphotograph of variolitic greenstone used in the estimation of finite strain. The scale bar is 0.5 cm long.

the near spherical shapes of varioles in specimens from areas of low D2 deformation.

The method

Each specimen was cut along three, mutually perpendicular planes, chosen so that one of the planes coincided with the S2 schistosity, and a second perpendicular to S2 containing the L2 lineation. These planes were used as initial estimates of the principal planes of the D2 strain ellipsoid and, since D2 is the most intense deformation phase, also the total finite strain ellipsoid. They were chosen because measurement on planes close to the principal planes improves the accuracy of the results. Each face was enlarged photographically (magnification of up to 5×) so that individual varioles were a minimum of 0.5 cm long. The long axis orientation of each variole was estimated by eye and measured to the nearest degree. Long and short axes were measured to within 0.01 mm (after magnification), from which the axial ratio was calculated.

The shape of an initially spherical particle after deformation defines the finite strain ellipsoid. Thus an estimate of finite strain can be obtained from a group of initially subspherical particles by arithmetically averaging their axial ratios. However, if the initial shape of the particles significantly departed from spherical, this leads to overestimation of the axial ratios (Lisle 1977) and a method which takes the initial variation in long axis orientation into consideration is required. Shimamoto & Ikeda (1976) have shown that, in the two-dimensional case, if the long axes of initially elliptical particles are randomly oriented,

Table 1. Results of average ellipse and arithmetic average methods applied to specimen 7, faces 1 to 3.

		Long axis orientation		Axial ratio	
	n	Ave. Ellipse	Arith. Ave.	Ave. Ellipse	Arith. Ave.
Face 1					
	20	9.5	10.0 ± 3.3	2.14	2.26 ± 0.17
	30	10.3	10.7 ± 2.7	2.13	2.24 ± 0.12
	40	10.9	11.3 ± 2.2	2.10	2.20 ± 0.10
	50	9.9	10.4 ± 2.0	2.14	2.25 ± 0.09
Face 2					
	20	−3.5	−3.5 ± 2.4	1.74	1.77 ± 0.06
	30	−0.0	0.0 ± 3.3	1.63	1.70 ± 0.06
	40	0.1	0.6 ± 2.9	1.62	1.69 ± 0.06
	50	1.6	1.8 ± 2.7	1.63	1.71 ± 0.06
Face 3					
	20	1.3	1.1 ± 2.0	3.22	3.39 ± 0.24
	30	1.2	1.1 ± 1.8	3.06	3.25 ± 0.20
	40	0.5	0.3 ± 1.5	3.15	3.35 ± 0.20
	50	0.5	0.4 ± 1.4	3.13	3.33 ± 0.17

the strain ellipse can be obtained from the deformed sample by averaging the components of the 2×2 matrices, each of which represents the shape and orientation of an elliptical particle.

For a test specimen of the variolitic greenstone, finite strain was estimated for each of the three faces using the two methods described above. The first method assumes that the particles were initially spherical and involves calculation of the arithmetic average of particle long axis orientations and axial ratios. Ninety-five percent confidence limits were calculated on the axial ratios (assuming a normal distribution) and long axis orientations (assuming a Von Mises distribution, method after Cheeney 1983). The second method (Shimamoto & Ikeda 1976) assumes that the particles were initially non-spherical and of random orientation. Each method was applied to 20, 30, 40 and 50 particles per face to test for the number of particles needed to give a satisfactorily reproducible result. The results of the two methods, shown in Table 1, agree to within the 95% confidence limits for the arithmetic method for both long axis orientations and axial ratios. There is, therefore, little error in assuming that the particles were initially spherical in shape. Most of the results for 20, 30, 40 and 50 particles show agreement within the 95% confidence limits for the arithmetic method, although an improvement in consistency was found if 30 or more particles were measured.

The arithmetic average of long axis orientations and axial ratios for a minimum of 30 particles wherever possible (all except three specimens) were calculated for each of the three faces from ten specimens of pillowed greenstone containing variolitic structures. The locations of these specimens are shown in Fig. 9 and listed in Table 2. Specimen 10 contains highly elongate varioles which have been folded by D3. In order to measure finite strain from this specimen, the lengths of the varioles were measured around F3 folds and their orientation assumed to be that of F3 fold long limbs. The finite strain result from this specimen therefore indicates largely D2 strain, the effects of F3 folding having been removed. The two-dimensional results were then combined using a method and computer program developed by Gendzwill & Stauffer (1981) to obtain the three-dimensional finite strain ellipsoid. In this method, the two-dimensional results are adjusted until a fit to a three-dimensional ellipsoid is obtained. The adjustments applied were found to lie within the 95% confidence limits on the two-dimensional data.

Finite strain analysis results

The results from the finite strain analysis of 10 specimens are listed in Table 2 and plotted in Fig. 14. A logarithmic plot of the axial ratios, a (maximum/intermediate) versus b (intermediate/

Table 2. Results of strain analysis for specimens 1 to 10.

Specimen	UTM coordinates	Axis lengths		Axis orientations	
		a	b	X	Z
1	VM488928	1.45	1.92	62 300	28 116
2	VM488929	1.57	1.79	25 124	46 244
3	VM493941	1.31	1.40	04 095	86 294
4	VM491941	1.15	1.39	24 266	60 123
5	VM486940	1.65	1.71	unknown orientation	
6	VM485939	1.47	2.03	50 355	02 086
7	VM485940	1.52	2.09	34 054	17 312
8	VM481943	1.57	1.68	66 104	05 004
9	VM478943	2.18	2.39	33 059	07 325
10	VM477943	3.33	4.38	36 059	06 154

minimum) is shown in Fig. 14(a). All specimens show nearly plane strain ($k = a/b = 1$) and lie consistently on the flattening side of the $k = 1$ line, with a wide range in intensity values. The maximum and minimum axes orientations are plotted on a lower hemisphere Lambert equal-area projection in Fig. 14(b) and show a wide scatter due to later F3 folding. The maximum axes show an arcuate trend similar to that for L2 lineations, which supports the assumption that L2 lineations parallel the D2 strain maximum.

The lowest strains, specimens 3 and 4, come from the central part of the eastern Joma Synform limb, whereas the highest strains, specimens 9 and 10, come from the western limb. This shows agreement with the qualitative estimations of S2 schistosity and S3 cleavage intensity throughout the lower greenstone. The finite strains measured (except for specimen 10) reflect the total strain experienced by the rock, i.e. the results of D1, D2 and D3 deformation phases. It has already been suggested, from fold interference patterns in the quartzitic phyllites, that D1 and D2 represent early and late stages of the same deformation phase and can therefore be considered equivalent to a single deformation from the point of view of strain. The specimens show varying degrees of S3 cleavage development (reflecting D3 deformation intensity) which is most intense in specimens 5, 8, 9 and 10. However, the finite strain results from these specimens do not depart significantly from the plane strain trend shown by specimens with low S3 cleavage development and this supports the suggestion that D3 deformation is coaxial with D1 and D2 deformations.

The near plane strain results for the finite strain analysis are consistent with a dominantly simple shear deformation mechanism for the main deformation (D1 and D2) with a NW–SE trending shear direction. This is also consistent with the distributions of folded L2 lineations around the Joma Synform which suggest a dominantly simple shear deformation mechanism during D3. The asymmetry of the Joma Synform indicates a south-easterly directed shear sense during D3 deformation, which is in agreement with the generally supposed direction of nappe movement during D1/D2 deformation phases. This suggests that D1, D2 and D3 deformations are not only coaxial but also share the same shear sense.

Discussion and conclusions

Way up of the Leipikvattnet Nappe in relation to the rest of the Middle Köli

Many of the Middle Köli Nappes have been established as comprising largely inverted stratigraphies. Stephens (1982) established the stratigraphy within the Stikke Nappe as, from oldest to youngest, phyllites and greenstones (Remdalen Group), metavolcanites (Stekenjokk volcanites) and calcareous phyllites (Blåsjö phyllites). This stratigraphy is dominantly inverted in the Stikke Nappe and partially inverted in the Gelvenåkko Nappe (Stephens & Reinsbakken 1981). In the Gjersvik Nappe, the Limingen Group calcareous phyllites are derived from, but structurally underlie, the Gjersvik metavolcanites, thus inferring an inverted stratigraphy for the Gjersvik Nappe (Halls et al. 1977). This is

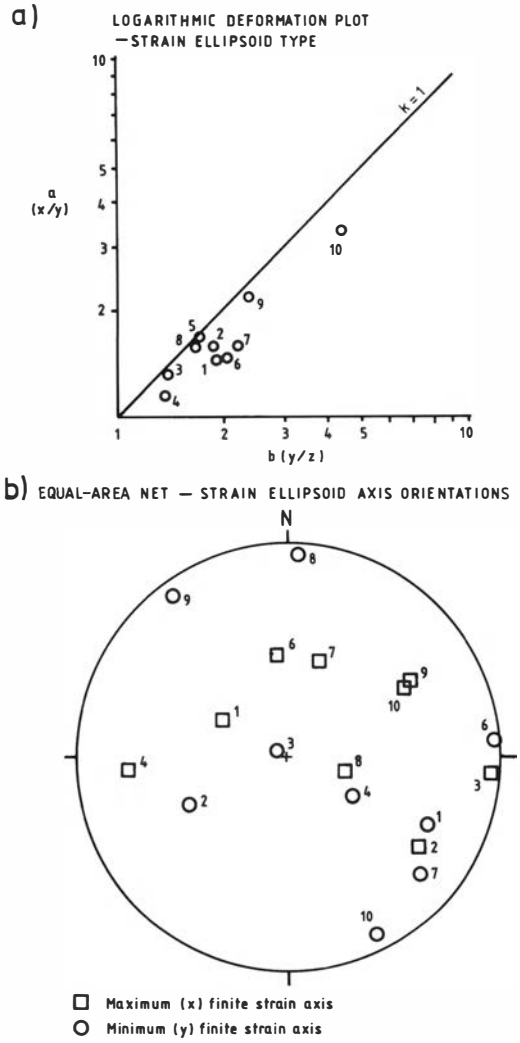

Fig. 14. (a) Deformation plot of axial ratio 'a' (maximum/intermediate) versus axial ratio 'b' (intermediate/minimum) for the finite strain results obtained from variolitic greenstone, specimens 1 to 10. (b) Stereoplot showing finite strain principal axis orientations for specimens 1 to 10.

supported by inverted stratigraphies found in the vicinity of the Skorovass (Halls et al. 1977) and Gjersvik (Reinsbakken 1986c) ore bodies.

Kollung (1979) suggested that within the Leipikvattnet Nappe the sequence quartzite, greenstone, phyllite was inverted (on the basis of way-up from a few pillow lava localities) and repeated by folding. This was seemingly supported by the work of Olsen (1980), which established that the stratigraphy within the Joma ore deposit was inverted. Stephens et al. (1985b) have correlated the Remdalen Group (Stikke Nappe) with the Røyrvik Group (Leipikvattnet Nappe) and tentatively correlate the Blåsjø Phyllite (Stikke Nappe) with the Brakkfjället Phyllite (Leipikvattnet Nappe), although the stratigraphic position of the Brakkfjället Phyllite remains highly uncertain (M. Stephens, pers. comm.). The structural relationship between the Brakkfjället Phyllite and the Røyrvik Group is uncertain (Stephens et al. 1985b), but if a stratigraphical relationship is assumed and a correlation of the Blåsjø and Brakkfjället Phyllites is correct, the location of the Brakkfjället Phyllite structurally below the Røyrvik Group would then infer an inverted stratigraphy within the Leipikvattnet Nappe.

The present study of the Joma area suggests that the stratigraphy (oldest) greenstone, quartzitic phyllite, graphitic phyllite (youngest) is repeated tectonically and that the bulk of the Leipikvattnet Nappe is the correct way up. The outcrop pattern in the middle greenstone indicates that the ore body lies in the overturned limb of a major F2 fold and thus the inversion of the ore body does not imply general inversion of the stratigraphy within the Leipikvattnet Nappe. Pillow lavas were generally found to be too deformed to be reliable as way-up indicators. It has also been tentatively suggested that not only the middle and upper greenstones but also the lower greenstone has a tectonic lower contact. If this is so, the Brakkfjället Phyllite is separated from the bulk of the Røyrvik Group by a thrust located at the base of the lower greenstone and, even allowing correlation of the Brakkfjället and Blåsjø Phyllites, need not imply inversion of the stratigraphy.

Correlation of deformation phases of the Joma area with the rest of the central Scandinavian Caledonides

Four phases of deformation have been recognized in the Joma area of which the first and second comprise the deformation associated with movement on the major and internal thrust planes. Within the central Scandinavian Caledonides in general, three to five deformation phases are recognized, indicating the heterogeneity of deformation on this scale. The Joma Synform (F3 in this study) belongs to a major set of upright folds (Zachrisson 1969) which can be traced throughout the central Scandinavian Caledonides

(Fig. 15). These folds trend N–S to NE–SW, show shallow northerly or southerly plunges and are associated with a variably developed crenulation cleavage, locally penetrative. In detail, these major folds are composed of a series of *en échelon* smaller folds which are characteristically impersistent along strike, examples of which are described from the Tärna Synform (Stephens 1977), Marsfjällen area (Trouw 1973), the Western Synform (Zachrisson 1969) and the Joma Synform (this study). These major folds can, however, be traced for distances of several hundreds of kilometres and they can therefore be used to correlate the deformation sequences of different areas within the central Scandinavian Caledonides.

The pre-D3 deformation sequence. – Between one and three phases are recognized as predating the major, N–S to NE–SW trending F3 folds.

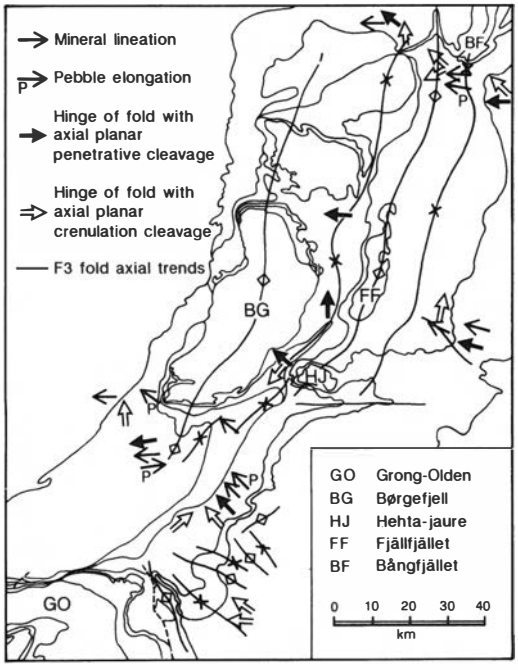

Fig. 15. Map of central Scandinavian Caledonides showing mineral lineations, pebble elongations and fold hinge trends for deformation associated with the movement on the major thrusts and major F3 fold trends, constructed from information in the literature mentioned in the text. Outlines of the nappe units are as for Fig. 1. Mineral lineations, pebble elongations and fold hinges associated with penetrative schistosity trend NW–SE to E–W, parallel to the generally supposed direction of nappe movement. Fold hinges associated with crenulation cleavage show variable trends, mostly N–S to NE–SW.

Throughout most of the area two phases are recognized, as in the Joma area, but in the Gjersvik Nappe in general only one has been found (Roberts 1979; Lutro 1979; Halls et al. 1977) and locally two (A. Reinsbakken, pers. comm.), while in the lower nappes of the Tärna–Björkvattnet and Kvarnsbergsvattnet areas (Stephens 1977; Sjöstrand 1978) three phases are identified. These deformation phases are associated with penetrative and crenulation cleavages subparallel to the major thrust planes and it is generally agreed that they are associated with major movement on these planes. Mineral and rodding lineations and pebble elongations (Lisle 1984 and others mentioned in the text above), after restoration to their pre-D3 orientations, trend E–W to NW–SE (Fig. 15) and are thought to reflect the movement direction of the nappe sequence.

Fold axes generally trend parallel to these lineations where associated with a penetrative schistosity, but show variable trends where associated with a crenulation cleavage, e.g. in the Marsfjällen area (Trouw 1973). This is thought to reflect the rotation of fold axes from perpendicular to parallel to the shear direction during progressive simple shear. In some areas, the crenulation cleavage can be traced laterally into a penetrative schistosity (Trouw 1973; Sandwall 1981) where earlier phases of deformation are preserved in garnet cores (Trouw 1973; Sjöstrand 1978; Lutro 1979) and as small-scale folds (Stephens 1977 and this study).

These phases of deformation can be interpreted as representing a repeated deformation cycle occurring within the same deformation event, in a similar way to that recorded in shear zones (Escher & Watterson 1974; Bell 1978; Platt 1983). The cycle begins with the development of folds with hinges at right angles to the shear direction with which a crenulation cleavage, initiated at approximately 45° to the shear plane, is associated. As deformation proceeds, the crenulation cleavage rotates towards the shear plane and becomes penetrative. At the same time, fold hinges are rotated into the shear direction. At a later stage this schistosity is itself folded and a second crenulation cleavage develops, marking another deformation cycle which, in time, obliterates the earlier fabric. The initiation of a new cycle (deformation phase) may be triggered by changes in dip of the thrust planes or cleavage planes (Bell 1978), caused, for example, by the

bending of nappes around others or wrapping of cleavage around competent masses. Platt (1983) also suggests that changes in strain rate can cause the foliation planes to rotate through the shear plane, thus initiating folds. In the Joma area, evidence of three such cycles has been identified, labelled D1, D2 and D3 phases. The variation in the number of cycles recognized in different areas within the central Scandinavian Caledonides suggests that deformation is heterogeneous on a regional scale and emphasizes the problems in attempting to correlate deformation phases over large distances on the basis of fabric type and style alone.

D3 and later deformation. – F3 and later folds fold the major thrust planes and therefore postdate the major nappe emplacement event. F3 folds occur as a conjugate set, the dominant fold of the set trending N–S to NE–SW, as already described. The subdominant set trends E–W to NW–SE with rather variable axial plane orientations and shallow west to NW plunges. This set is best developed east and south of the Joma area, where dome-and-basin structures are locally developed (Halls et al. 1977; Sjöstrand 1978; Sandwall 1981).

Superimposed on and therefore postdating the regional NE–SW trending folds is a set of folds and kinks with subhorizontal axial planes and variable, but commonly NE or SW plunges which correlate with D4 structures of the Joma area. This deformation varies widely in intensity from sporadic minor kinks or weakly developed crenulation cleavage to near-isoclinal folds of chevron style with well-developed crenulation cleavage, in a few places penetrative. In areas where D4 structures are only weakly developed, they are most commonly observed on steep standing schistosities (Stephens 1977; Sjöstrand 1978). Wherever observed, D4 folds verge down the dip of the previous schistosity and therefore show opposite vergence on east and west limbs of many of the major F3 folds (Zachrisson 1969).

In the Joma area, D4 structures were found to have a complementary spatial relationship with D3 deformation, being best developed in and adjacent to the Gjersvik Nappe (Roberts 1979; Lutro 1979) where D3 deformation is weak. From descriptions of the structure of the Lierne district (Aukes et al. 1979), it is possible that D3 and D4 structures show a similar relationship in the Köli and Seve Nappes there. Close to tight folds with subhorizontal axial planes (F3 of Aukes 1979) in the Offerdal Nappe and in the Lower and Upper Köli sequence probably correspond to F4 folds of the Joma area. This deformation is described as most intense in the Lower Köli, where a strong crenulation cleavage is developed. In the Seve Nappe to the east, no mention is given by Aukes et al. (1979) of flat-lying folds, but their Group II folds, open folds with steeply dipping axial planes which fold the regional foliation, can be interpreted as corresponding to F3 of the Joma area. Westwards from the Lower Köli sequence, F4 folds become more open and isoclinal folds, dipping moderately to steeply NW (their F2), become dominant. These could represent F2 or F3 folds described here. It thus appears that there is a zone of flat-lying folds (D4?) trending approximately NE–SW from the pronounced bend in the Grong–Olden Culmination west of Nordli which may be flanked by zones where NW–SE trending, moderately to steeply dipping folds (D3?) are developed. If this is the case, it may be that the spatial relationship between D3 and D4 deformation described in the Joma area is a more general phenomenon.

Relationship and possible origin of F3 and F4 folds

F3 folds deform the major thrust planes and therefore postdate the main thrusting event at the structural level exposed today. Analysis of folded L2 lineation patterns and finite strain from the Joma area suggest that F3 folding was generated by dominantly simple shear and it is suggested that D3 deformation is a continuation of the deformation that occurred during the main thrusting event. The cause of cessation of movement on the major thrust planes is unknown but could have been caused by, for instance, a decrease in fluid pressure resulting from a decrease in overburden thickness or rotation of the thrust planes into an unfavourable orientation.

Within the central Scandinavian Caledonides, the majority of large-scale F3 folds are described from the region to the east of the broad antiformal structure passing through the Børgefjell massif (Fig. 1), and this suggests the possibility that they may be associated with late movement of this massif. The Børgefjell massif is one of a series of basement windows which form a zone immediately to the east of the Norwegian/Swedish border. The zone includes, to the south, the Tomerås Antiform and the Grong–Olden Cul-

mination, and to the north, the Bångfjället, Nasafjället and Rombak-Sjangeli windows (Stephens et al. 1985b). The precise tectonic nature of most of these windows is uncertain, but in some evidence exists of an, at least partially, allochthonous character. The presence of thrusts internal to the Nasafjellet window (Thelander et al. 1980) shows that it contains allochthonous components and it has also been suggested that the Børgefjell massif may be allochthonous on the basis of strong Caledonian deformation (Greiling 1981) and a lack of any negative residual gravity anomaly (Gabrielsen et al. 1981). A rise of the Børgefjell massif, either by ductile diapiric rise of the basement or a late eastward movement of the massif on a deep-seated thrust plane, would tend to steepen the dip of the major thrust planes, rendering them less effective for accommodating subhorizontal compression. The resulting deformation either from a direct push provided by the rising massif or by gravity sliding of the nappe pile eastwards off the rising dome, would then lead to the development of large-scale, upright folds whose axes trended approximately perpendicular to the direction of maximum compression. The location of F3 folds predominantly to the east of the Børgefjell massif would suggest that some lateral, easterly directed, as well as vertical movement occurred. The evidence that the Joma Synform developed under simple shear deformation also favours the interpretation that the massifs are underlain by a deep-seated thrust along which late movement took place.

The spatial relationship between D3 and D4 intensity in the Joma area, described above, has led to the suggestion that these two deformation phases are closely linked. In contrast to F3 folds, F4 folds do not form major structures. Their consistent down-dip sense of overturning, regardless of dip direction, and their subhorizontal axial plane orientation, makes it difficult to relate them to any late movements associated with the main thrusting event, as has been suggested above for F3 folding. Late tectonic folds of similar style and orientation are also found in the Trondheim region where they too are consistently overturned down-dip. The subhorizontal attitude of F4 axial planes indicates an approximately vertical direction of maximum compression, which with the sense of overturning down-dip is consistent with gravity as the driving force and it has been suggested (Roberts 1967; Roberts et al. 1970) that these structures are the result of gravitational collapse of the nappe pile after the relaxation of the compression responsible for the development of the Caledonides. In the Kopperå–Riksgrensen area, Roberts (1967) postulates an origin by gravitational sliding towards the deep rooted core of the early Stjørdalen fold. Although correlation of deformation phases across the Grong–Olden Culmination is problematic, the similarity in style, orientation, intensity and the late timing suggest a similar origin. Roberts (pers. comm. in Kollung 1979) consequently suggested that the structures north of the Grong–Olden Culmination are also of gravitational origin, forming on the flanks of pre-existing folds. Stephens (1977) found that late shallowly dipping, conjugate sets of kinks in the Tärna/Björkvattnet area implied a steeply plunging orientation for the maximum compression during their formation and also postulated an origin involving gravitational collapse.

Previous to D4 deformation, fold and thrust structures indicated an approximately horizontal orientation for the maximum compression direction and thus between the third and fourth deformation the horizontal stress was reduced to a level less than that induced by the overburden. However, because all rocks of the Caledonides do not show well developed D4 structures, the resulting differential stresses became large enough to generate significant deformation only in selected areas. It has been suggested that F3 folds could have resulted from late stage movements of the Børgefjell massif which generated compression east of the uplift zone. Such an uplift would also have resulted in reduced horizontal compression overlying the massif. If the horizontal compression were reduced sufficiently, the vertical stress due to overburden pressure could become the maximum stress direction and have led to the development of folds with subhorizontal axial planes, the gravitational collapse mechanism described by Roberts (1967).

In this model, the relative timing between the development of steeply dipping, NE–SW trending and subhorizontal folds is dependent on the movement direction of the massifs and the pre-existing stress system. It is likely that the stress system prior to the development of F3 folds was one of horizontal compression. It may therefore have required little extra compression to initiate the steeply dipping folding to the east. However, to reduce the horizontal compression to less than the overburden pressure by an amount large enough to generate subhorizontal folds probably

comprised a greater change in the stress system. Thus folds due to gravitational forces would be likely to postdate the steeply dipping, NE–SW trending folds. As the subhorizontal compressional stresses that were responsible for the development of the Caledonian orogeny waned, all rocks would eventually experience a maximum vertical stress due to overburden. However, as subhorizontally oriented minor structures are poorly developed throughout most of the central Scandinavian Caledonides, it seems that, by this time, the overburden thickness had been reduced by erosion so that the vertical stress was insufficient and temperatures too low to allow significant ductile deformation.

It is suggested, therefore, that reactivation of movement involving the Børgefjell massif occurred late in the history of the central Scandinavian Caledonides. These movements created compression, most pronounced to the east of the massif, and probably tilted the major thrust planes so that they were no longer effective. This resulted in the development of major upright, NE–SW trending folds, largely to the east of the major Børgefjell massif. Movement of the massif caused reduced horizontal compression over its crest so that vertical stress due to overburden became the maximum stress which, in the Gjersvik Nappe of the Joma area, became large enough to cause the development of folds with subhorizontal axes. The relative timing of D3 and D4 deformation phases can be explained by the magnitude of the changes in the stress system needed to initiate these deformations. From descriptions of late, subhorizontal folds in the Lierne district (Aukes et al. 1979) and the Trondheim region (Roberts 1967; Roberts et al. 1970), deformation associated with subhorizontal folds is widespread throughout at least the central Scandinavian Caledonides. It is not known whether they show a similar relationship with the previous fold phase in these areas, but in both the Lierne and the Kopperå–Riksgrensen areas they occur in areas adjacent to basement massifs (the Grong–Olden Culmination and Tommeråsen Antiform respectively). It may be, therefore, that late uplift of basement massifs also played a role in the development of subhorizontally oriented folds in other areas.

Acknowledgements. – The above work was completed as part of a project on the Joma ore deposit at the Geologisk Institutt, N.T.H., Trondheim, Norway, while the author was in possession of a N.T.N.F. post-doctoral fellowship. The project was financed by N.T.N.F., grant number NB10.15042 and by Grong Gruber A/S. I would like to thank Professor F. M. Vokes, A. Reinsbakken, A. Haugen and R. Horbach for their help and scientific discussion during the project. I also thank M. B. Stephens, A. Reinsbakken, Professor F. M. Vokes and A. Haugen for critically reading the manuscript.

Manuscript received January 1989

References

Aukes, P. G., Reymer, A. P. S., de Ruiter, G. W. M., Stel, H. & Swart, H. T. 1979: The geology of the Lierne District, northeast of the Grong Culmination, central Norway. *Norges geologiske undersøkelse 354,* 115–129.

Bell, T. H. 1978: Progressive deformation and reorientation of fold axes in a ductile mylonite zone: the Woodroffe thrust. *Tectonophysics 44,* 285–320.

Cheeney, R. F. 1983: *Statistical Methods in Geology.* George Allen & Unwin, London. 169 pp.

Escher, A. & Watterson, J. 1974: Stretching fabrics, folds and crustal shortening. *Tectonophysics 22,* 223–231.

Fossen, H. & Kollung, S. 1988: Jomafjellet berggrunnskart 1924, 1, 1: 50 000, foreløpig utgave Norges geologiske undersøkelse.

Gabrielsen, R. H., Ramberg, I. B., Mørk, M. B. E. & Tveiten, B. 1981: Regional geological, tectonic and geophysical features of Nordland, Norway. *Earth Evol. Sci. 1,* 14–26.

Gendzwill, D. J. & Stauffer, M. R. 1981: Analysis of triaxial ellipsoids; their shapes, plane sections and plane projections. *Mathematical Geology 13,* 135–152.

Greiling, R. 1981: Caledonian thrusting in the basement rocks of the Børgefjell window (north-central Scandinavian Caledonides) as related to major nappe transport. (Abstract) *Terra Cognita 1,* 47.

Häggbom, O. 1978: Polyphase deformation of a discontinuous nappe in the central Scandinavian Caledonides. *Geologiska Föreningens i Stockholm Förhandlingar 100,* 349–354.

Halls, C., Reinsbakken, A., Ferriday, I. & Haugen, A. 1977: Geological setting of the Skorovass orebody within the allochthonous volcanic stratigraphy of the Gjersvik Nappe, central Norway. *Geological Society London Special Publication 7,* 128–151.

Kollung, S. 1979: Stratigraphy and major structures of the Grong district, Nord-Trøndelag. *Norges geologiske undersøkelse 354,* 1–51.

Kollung, S. 1979: Unpublished 1: 50 000 map of the Huddingsvatnet area.

Lisle, R. J. 1977: Estimation of the tectonic strain ratio from the mean shape of deformed elliptical markers. *Geologie en Mijnbouw 56,* 140–144.

Lisle, R. J. 1984: Strain discontinuities within the Seve–Köli Nappe complex, Scandinavian Caledonides. *Journal Structural Geology 6,* 101–110.

Lutro, O. 1979: The geology of the Gjersvik area, Nord-Trøndelag, central Norway. *Norges geologiske undersøkelse 354,* 53–100.

Marshall, B. in press. 'Pseudostratigraphy' and thrusting in relation to the structural evolution of the Joma ore body, North Trøndelag, Norway. *Ore Geology Review.*

Odling, N. E. (1988): Deformation of the Joma sulphide deposit, Caledonides of N. Trøndelag, Norway. *Proceedings of the Seventh Quadrennial IAGOD Symposium,* 513–524. E. Schweizerbart'sche, Stuttgart.

Olsen, J. 1980: Genesis of the Joma stratiform sulphide deposit, central Scandinavian Caledonides. *Proceedings of the Fifth Quadrennial IAGOD Symposium*, 745–757. E. Schweizerbart'sche, Stuttgart.

Platt, J. P. 1983: Progressive refolding in ductile shear zones. *Journal Structural Geology 5*, 619–622.

Ramberg, I. B. 1981: The Brakkfjället tectonic lens: evidence of pinch-and-swell in the Caledonides of Nordland, north central Norway. *Norsk Geologisk Tidsskrift 61*, 87–91.

Ramsay, J. G. 1967: *Folding and Fracturing of Rocks*. McGraw-Hill, London, 562 pp.

Reinsbakken, A. 1986a: The geology of the Joma sulphide deposit, Nord-Trøndelag, Norway. Part II: Stratigraphical, petrological, mineralogical and geochemical studies of the ore and its surroundings. Unpublished report, Geologisk Institutt, N.T.H., University of Trondheim. 70 pp.

Reinsbakken A. 1986b: The Joma Cu–Zn massive sulphide deposit hosted by mafic metavolcanites. *In* Stephens, M. B. (ed.): Stratabound sulphide deposits in the central Scandinavian Caledonides. *Sveriges geologiska undersökning Ca60*, 45–49.

Reinsbakken, A. 1986c: The Gjersvik Cu–Zn massive sulphide deposit in a bimodal metavolcanic sequence. *In* Stephens, M. B. (ed.): Stratabound sulphide deposits in the central Scandinavian Caledonides. *Sveriges geologiska undersökning Ca60*, 50–54.

Reinsbakken, A. & Stephens, M. B. 1986: Lithology and deformation in the massive sulphide-bearing Gelvenåkko and Leipikvattnet Nappes, Upper Allochthon. *In* Stephens, M. B. (ed.): Stratabound sulphide deposits in the central Scandinavian Caledonides. *Sveriges geologiska undersökning Ca60*, 42–45.

Roberts, D. 1967: Structural observations from the Kopperå–Riksgrense area and discussion of the tectonics of Stjørdalen and the N.E. Trondheim region. *Norges geologiske undersøkelse 245*, 64–122.

Roberts, D. 1979: Structural sequence in the Limingen-Tunnsjøen area of the Grong district, Nord-Trøndelag. *Norges geologiske undersøkelse 354*, 101–114.

Roberts, D., Springer, J. & Wolff, F. C. 1970: Evolution of the Caledonides in the northern Trondheim region, Central Norway: a review. *Geological Magazine 107*, 133–145.

Sandwall, J. 1981: Caledonian geology of the Jofjället area, Västerbotten County, Sweden. *Sveriges geologiska undersökning C778*, 105 pp.

Shimamoto, T. & Ikeda, Y. 1976: A simple algebraic method for strain estimation from deformed ellipsoidal objects. I. Basic theory. *Tectonophysics 6*, 315–337.

Sjöstrand, T. 1978: Caledonide geology of the Kvarnsbergsvattnet area, Northern Jämtland, central Sweden: stratigraphy, metamorphism and deformation. *Sveriges geologiska undersökning C735*, 107 pp.

Stephens, M. B. 1977: Stratigraphy and relationship between folding, metamorphism and thrusting in the Tärna–Björkvattnet area, northern Swedish Caledonides. *Sveriges geologiska undersökning C726*, 146 pp.

Stephens, M. B. 1982: Field relationships, petrochemistry and petrogenesis of the Stekenjokk volcanites, central Swedish Caledonides. *Sveriges geologiska undersökning C786*, 111 pp.

Stephens, M. B. 1986: Metallogeny of stratabound sulphide deposits in the central Scandinavian Caledonides. *In* Stephens, M. B. (ed.): Stratabound sulphide deposits in the central Scandinavian Caledonides. *Sveriges geologiska undersökning Ca60*, 5–16.

Stephens, M. B. & Gee, D. G. 1985: A tectonic model for the evolution of the eugeoclinal terranes in the central Scandinavian Caledonides. *In* Gee, D. G. & Sturt, B. A. (eds.): *The Caledonian Orogen: Scandinavia and Related Areas*, 953–978. Wiley, New York.

Stephens, M. B., Furnes, H., Robins, B. & Sturt, B. A. 1985a: Igneous activity within the Scandinavian Caledonides. *In* Gee, D. G. & Sturt, B. A. (eds.): *The Caledonian Orogen: Scandinavia and Related Areas*, 623–656. Wiley, New York.

Stephens, M. B., Gustavson, M., Ramberg, I. B. & Zachrisson, E. 1985b: The Caledonides of central-north Scandinavia – a tectonostratigraphic overview. *In* Gee, D. G. & Sturt, B. A. (eds.): *The Caledonian Orogen: Scandinavia and Related Areas*, 135–162. Wiley, New York.

Stephens, M. B. & Reinsbakken, A. 1981: Excursions in the Scandinavian Caledonides. Successions related to island arcs in the Köli Nappes, central Scandinavian Caledonides. U.C.S. Excursion Guide No. B14, Uppsala Caledonide Symposium (UCS).

Thelander, T., Bakker, E. & Nicholson, R. 1980: Basement-cover relationships in the Nasafjället Window, central Swedish Caledonides. *Sveriges geologiska undersökning 102*, 569–580.

Trouw, R. A. J. 1973: Structural geology of the Marsfjällen area, Caledonides of Västerbotten, Sweden. *Sveriges geologiska undersökning C689*, 115 pp.

Zachrisson, E. 1964: The Remdalen syncline, stratigraphy and tectonics. *Sveriges geologiska undersökning C596*, 53 pp.

Zachrisson, E. 1969: Caledonian geology of northern Jamtland, southern Västerbotten. *Sveriges geologiska undersökning C644*, 33 pp.